Aero-Structural Wind Tunnel Experiments with Elastic Wing Models at High Reynolds Numbers (HIRENASD - ASDMAD)

J. Ballmann[1], A. Boucke[2], B.-H. Chen[3], L.Reimer[4], M. Behr[5], A. Dafnis[6], C. Buxel[7], S. Buesing[8], H.-G. Reimerdes[9], K.-H. Brakhage[10], H. Olivier[11]
All RWTH Aachen University, Germany

M. Kordt[12] , J. Brink-Spalink[13], F. Theurich[14], A. Büscher[15]
Airbus GmbH, Germany

The SFB 401 *Flow Modulation and Fluid-Structure Interaction at Airplane Wings* at RWTH Aachen has first performed experiments in the *European Transonic Windtunnel* (ETW) with a swept elastic clean wing model in its central project *High Reynolds Number Aero-Structural Dynamics* (HIRENASD). Mach numbers were in the transonic regime. The model has been excited for vibration applying span-wise acting interior force couples in the wing root region. The structure is made from linear elastic material and consists of the wing model and its suspension in the wind tunnel. In the follower project ASDMAD the model has been shortened in the tip range to be equipped and tested in ETW in succession with two different winglets. Data from one series of experiments is already available and is used to compare with HIRENASD results for corresponding wind tunnel conditions. In the HIRENASD project, the analysis of the raw data for quasi-stationary tests brought to light weak upstream running pressure waves behind shocks or even upstream running shocks forming from steepening compression waves when the transonic regime is still being established. This phenomenon was not observed as clearly in the data from the ASDMAD experiments. For excited vibration the results are more comparable. A convincing argument was elaborated from the HIRENASD data, why artificial transition in aero-elastic experiments at low Reynolds number can not replace experiments at realistic Reynolds numbers.

[1] Professor, retired, Mechanics Department (LFM), Schinkelstrasse 2, 52062 Aachen, Germany, AIAA member.
[2] Senior Scientist, Mechanics Department (LFM), Schinkelstrasse 2, 52062 Aachen, Germany.
[3] Research Assistant, Chair of Computational Analysis of Technical Systems (CATS), Schinkelstrasse 2, 52062 Aachen, Germany.
[4] Research Assistant, Chair of Computational Analysis of Technical Systems (CATS), Schinkelstrasse 2, 52062 Aachen, Germany.
[5] Professor, Chair of Computational Analysis of Technical Systems (CATS), Schinkelstrasse 2, 52062 Aachen, Germany.
[6] Senior Scientist, Institute of Lightweight Structures (ilb), Wüllnerstrasse 7, 52062 Aachen, Germany.
[7] Research Assistant, Institute of Lightweight Structures (ilb), Wüllnerstrasse 7, 52062 Aachen, Germany.
[8] Research Assistant, Institute of Lightweight Structures (ilb), Wüllnerstrasse 7, 52062 Aachen, Germany.
[9] Professor, Institute of Lightweight Structures (ilb), Wüllnerstrasse 7, 52062 Aachen, Germany.
[10] Senior Scientist, Institute for Applied Mathematics (IGPM), Templergraben 55, 52062 Aachen, Germany.
[11] Professor, Shock Wave Laboratory, Schurzelter Strasse 35, 52074 Aachen, Germany.
[12] Project Manager, Airbus Deutschland GmbH, Kreetslag 10, 21129 Hamburg, Germany
[13] Project Manager, Airbus Deutschland GmbH, Kreetslag 10, 21129 Hamburg, Germany
[14] Specialist, Airbus Deutschland GmbH, Kreetslag 10, 21129 Hamburg, Germany
[15] Specialist, Airbus Deutschland GmbH, Kreetslag 10, 21129 Hamburg, Germany

Nomenclature

α	=	angle of attack
A_{ref}	=	wing reference area
ACC	=	acceleration
BFy	=	wing normal force component
c	=	chord
c_{ref}	=	aerodynamic mean chord
c_p	=	pressure coefficient
E	=	Young's modulus of model material
f	=	frequency
F_x	=	X component of force
F_y	=	Y component of force
F_z	=	Z component of force
η	=	non-dimensional span
HV1	=	voltage in piezoelectric stack 1
Ma	=	Mach number
p_{tot}	=	total pressure
q, Q	=	dynamic pressure
Re, Re_c	=	Reynolds number
T_{tot}	=	total temperature
x/c	=	non-dimensional chord
ξ, D	=	damping coefficient

I. Introduction

The High Reynolds Number Aero-Structural Dynamics (HIRENASD) project was initiated in 2004 at RWTH Aachen University with financial support from the German Research Foundation (DFG) within the frame of the Collaborative Research Center "Flow Modulation and Fluid-Structure Interaction at Airplane Wings" (SFB 401)[1]. It has been devoted to the analysis of stationary and non-stationary aero-elastic experiments with a supercritical elastic wing model in the transonic regime at Reynolds numbers which are realistic for large passenger aircraft in cruise flight. Experiments were performed in the European Transonic Windtunnel (ETW) under cryogenic conditions in nitrogen gas. Since freely accessible experimental aero-elastic data for university research was not available at the time when HIRENASD was started and is still rare, an appropriate modern data base had to be created through the project.

Usually dynamical wind tunnel experiments with elastic wing models have been conducted mainly at Reynolds numbers which are about one order of magnitude less than in cruise flight of large aircraft[2]. Only for a rigid airfoil, oscillating with prescribed frequency, experiments in transonic flow at high Reynolds numbers had been made earlier at NASA LaRC [3] for buffet analysis, whereby cryogenic wind tunnel conditions made the high Reynolds numbers feasible too.

Before the SFB 401 ended after the admissible maximum funding time of twelve years at the end of 2008 the HIRENASD research program has been continued in a so-called transfer project ASDMAD with funding from DFG, Airbus Germany and RWTH Aachen University, Germany. The new project includes two other series of Aero-Structural Dynamics (ASD) experiments in ETW with the HIRENASD wing model modified at wing tip by two types of winglets, one with fixed geometry and another equipped with a movable flap. For these modifications SFB 401 placed at disposal the elastic wing model, which was developed in the HIRENASD project, including the implemented measuring equipment. The model has been shortened in the tip range for winglet attachment whereby the former span after mounting of the winglet has been maintained. The first series of experiments (ASDMAD-1, winglet with fixed geometry) took already place in 2010, the second series of experiments which includes vibration influencing by the moveable winglet flap is now scheduled for 2011. Sensors and sensor positions have been maintained, except for pressure section 7 which is now occupied by a winglet.

In chapter II of the paper the wind tunnel model, its measuring equipment and test envelopes are shortly described. For more details about the HIRENASD model the reader is referred to the cited literature and to the HIRENASD homepage http://www.lufmech.rwth-aachen.de/HIRENASD/[4]; where all geometrical and physical properties of the model, including all sensor positions and wind tunnel conditions as well as a complete list of the experiments, are presented. Furthermore, there are computational grids for the wing structure and the flow field provided for downloading which can considerably facilitate numerical simulations of the ASD experiments by interested researchers.

In chapter III of the paper, selected quasi-stationary experiments from HIRENASD and ASDMAD-1 are regarded with respect to non-stationary contents of the raw data. For the HIRENASD raw data the analysis brought to light periodically upstream running small amplitude pressure waves in the subsonic region of the wing surface, also behind shocks when the transonic regime was well established. This type of waves has first been experimentally analysed by Tijdemann[5] and had also been observed in DNS simulations reported in ref. 6 considering the HIRENASD pre-tests with a BAC 3-11 airfoil[10] in the Ludwieg-type cryogenic wind tunnel KRG, Göttingen. These pre-tests were done to check the pressure measurement equipment under cryogenic conditions as foreseen for the HIRENASD tests in ETW. The observed wave phenomenon was interpreted as the result of small vortices in the surface boundary-layer which trigger the waves through the periodical vortex detachment from the trailing edge. The KRG experiments were also discussed in ref. 7. Those waves could be visualized in transonic shock tube flow[8] and simulated applying DNS. In the HIRENASD experiments even periodically upstream running shocks are observed which form with a clear frequency from steepening compression waves behind the mid-chord.

In chapter IV results from selected experiments with vibration excitation from the HIRENASD and ASDMAD-1 tests are discussed regarding filtering by means of Fourier analysis and data reduction.

II. Elastic Wing Models for Aero-Structural Dynamics Tests in ETW and Test Conditions

A. HIRENASD Wing Model

The wing model corresponds to the SFB 401 clean wing reference configuration, which has a plan-form as typical for large passenger transport aircraft[9], with 34^o backward sweep angle and the supercritical wing profile BAC 3-11 reported in AGARD-AR-303[10], which has been arranged for cruise flight, see Fig. 1. The wetted part of the complete elastic wind tunnel assembly has a span of 1.375m. The aerodynamic reference area and mean chord of the wing model are A_{ref}=0.3926m² and c_{ref}=0.3445m.

In the evaluation process of the stationary and dynamic experiments in ETW for natural frequencies and mode shapes of the elastic wing configuration mounted in the measuring section of ETW, it was recognised that not only the elasticity of the wing model is to be considered. A suitable description of the elastic properties has to include the elasticity of the wing clamping, the balance and the ETW adapter as well, which is used to fix the balance at the wind tunnel wall. All elastic components taken into account for modelling the elastic assembly are shown in the left upper picture in Fig. 2. Depicted in the five other pictures of Fig. 2 are presentations of mode shapes from the final approach for a well suited beam model C for the configuration, which compares well to both a 3D Tet10 model of the complete elastic assembly and the measurements. Figure 3 shows for seven modes of flap bending and torsion the shapes reconstructed from accelerometer measurements at 10 different locations in the wing during vibration excitation with a frequency close to the first mode frequency[11]. At the same time the other natural modes are excited as well by inherent stochastic flow disturbation such that data can be evaluated also for other modes as shown in Fig. 3.

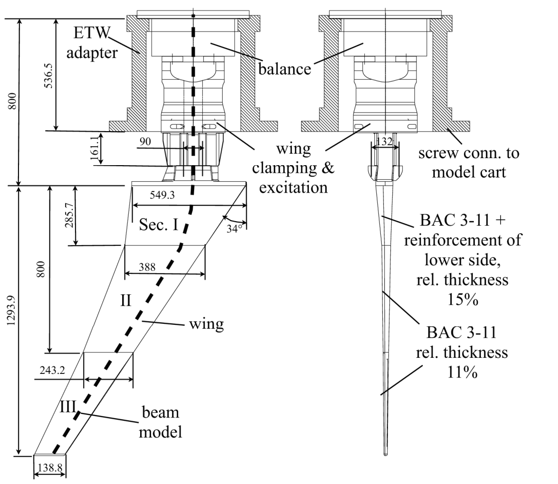

Figure 1. HIRENASD wing model. Views on the pressure side (left) and in flow direction (right).

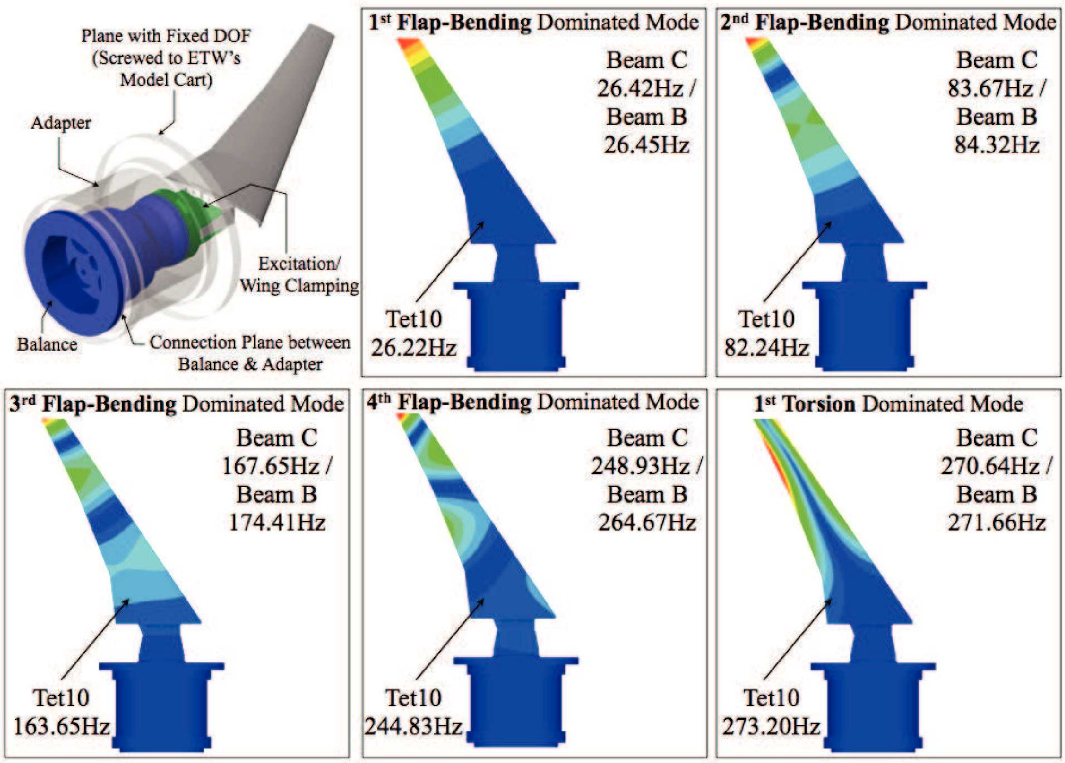

Figure 2. Natural modes and frequencies of the complete elastic wing assembly including balance and adapter from FEM computations. Tet10 volume model. Beams B, C Timoshenko models.

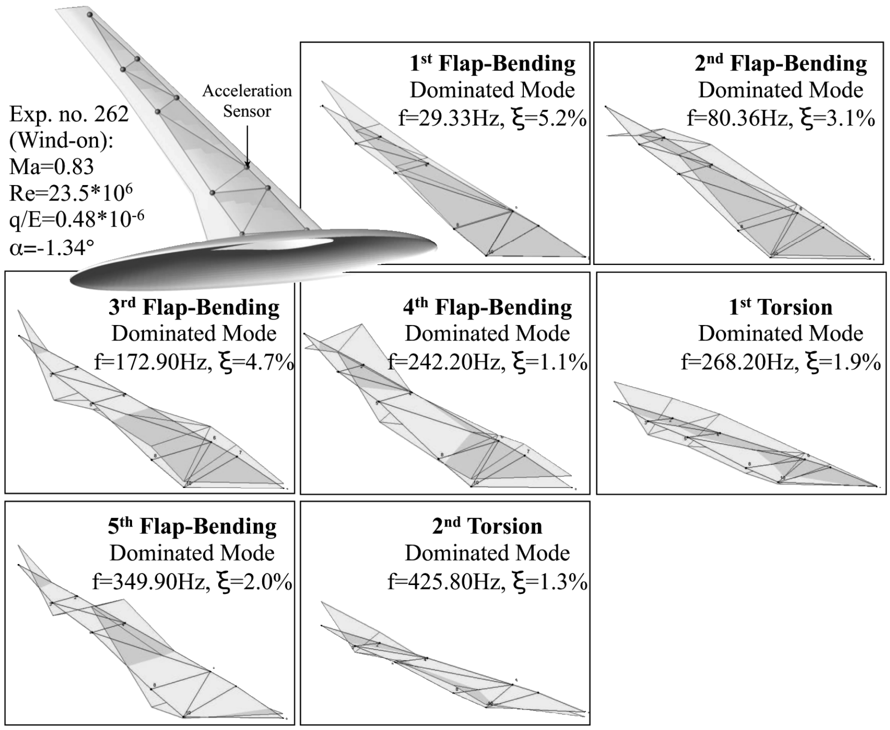

Figure 3. Natural modes determined from stochastic excitation during wind tunnel test.

B. Wing Tip Modifications for the Transfer Project ASDMAD

For the ASDMAD project the HIRENASD model was placed at disposal including its implemented measurement technique. The wing has been shortened in the tip range to be equipped and tested in ETW in succession with two different winglets of which the first one is larger and has a rigid geometry, while the second one has a non-rigid geometry due to a moveable aerodynamic control surface (ACS)[14]. Figure 4 exhibits on the left the HIRENASD wing model in a view on the pressure side. Its tip has been removed according to the shaded region in the figure, and a common interface for overlapping fixing of each of the winglets has been provided. On the right part of the figure both winglets are depicted together to explain their different surface geometry. The former wing span is maintained for the two resulting configurations[12,13]. The quantities c_{ref} and A_{ref} from the HIRENASD model are maintained. Figure 5 shows on the left a photograph of the ASDMAD-1 modification with the rigid winglet in the test section of ETW and on the right the winglet with ACS (dark coloured). The result of a design supporting computation using the CASD package SOFIA[1,11,12] is shown for one of the wind tunnel conditions.

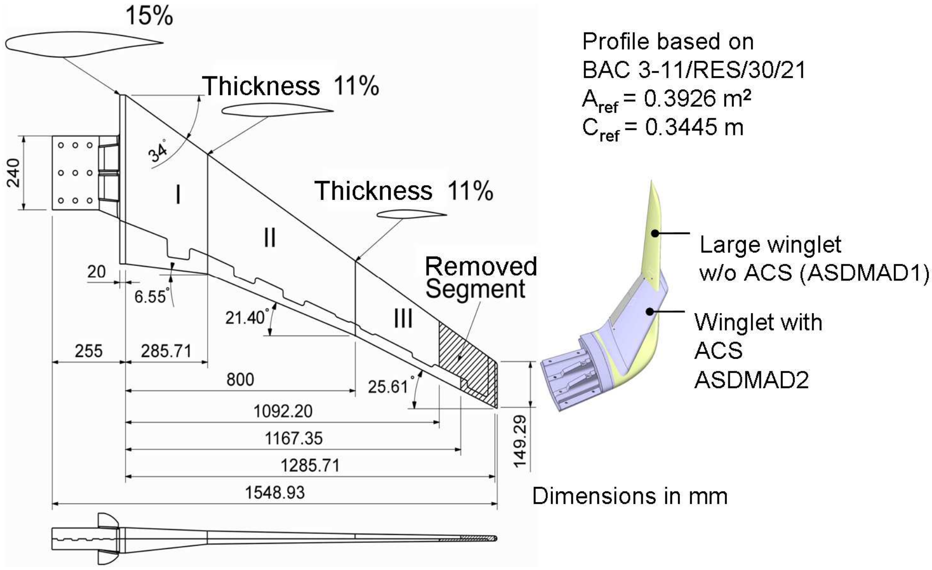

Figure 4. Wing modification to attach different winglets (left: view on the pressure side). Right: Winglets to be attached successively, view on the suction side.

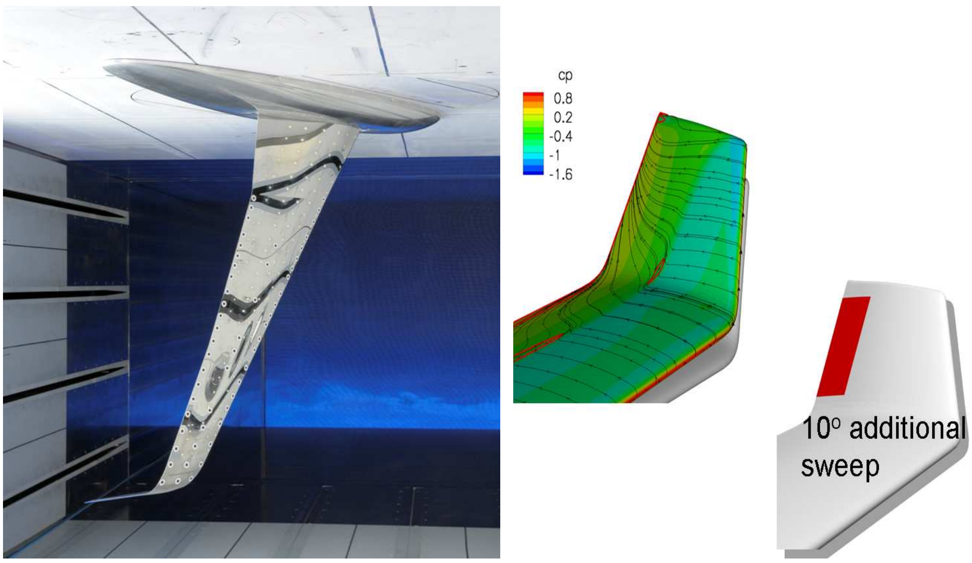

Figure 5. Left: Modified wing model ASDMAD-1 in wind tunnel. Slots in the side wall open. Right: Wing tip modification for ASDMAD-2. Middle: CASD result for winglet with ACS, Re=23.5·10^6, q/E=0.34 ·10^{-6}, α=3°.

C. Measuring Equipment

The HIRENASD model was equipped with five different measurement techniques: A new piezoelectric wind tunnel balance, an optical surface pattern tracking system using markers, acceleration sensors, strain gauges and a large number of Kulite pressure sensors distributed in seven wing sections. The model has been excited for vibration applying span-wise acting interior force couples in the wing root region. This paper gives only a short overview, a more detailed description of the measurement techniques and excitation can be found in ref. 15 and 4.

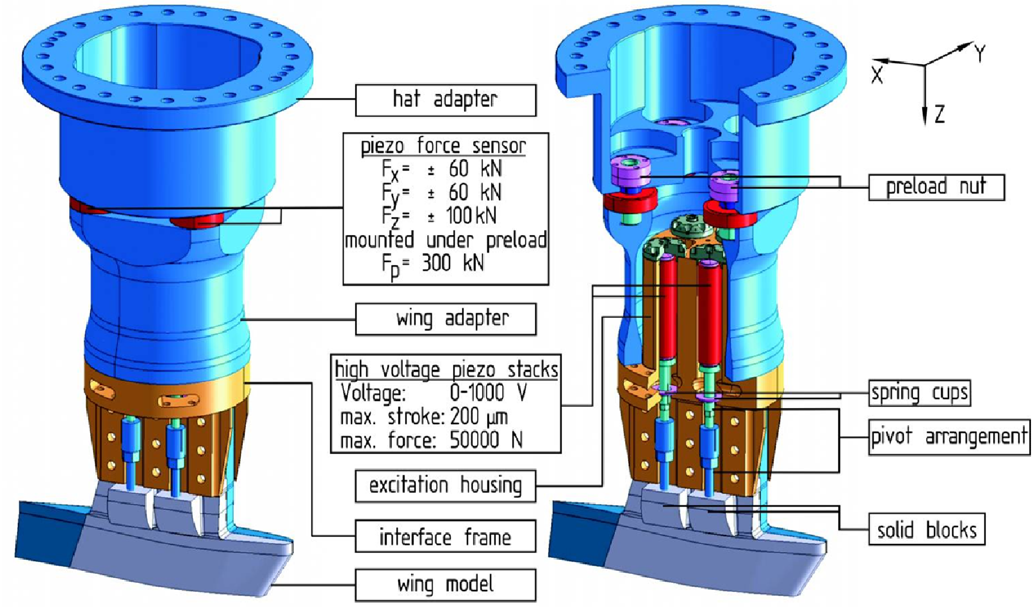

Figure 6. Balance (on top), vibration excitation mechanism (middle) with force transmitters to prominent wing noses (solid blocks) and wing clamping.

As already mentioned a new 6-components wind tunnel balance based on four piezoelectric load cells has been designed and built for force measurement in the dynamical aero-elastic experiments because the installed balance in ETW had been originally designed for precise measurement in stationary testing. It is by far not stiff enough for dynamic measurements. The new balance is very stiff, the frequencies of its lowest natural modes are beyond 800Hz[15] whereas the highest planned excitation frequency in the HIRENASD experiments was below 300Hz. The balance forms an integrated part with the housing of the piezoelectric excitation mechanism and the clamping of the wing model, shown in Fig. 6. Forced vibration of the wind tunnel model is realised by dynamic force couples made up by four span-wise directed forces which are applied at prominent noses of the wing root (named solid blocks in Fig. 6). The whole mechanism is integrated in a housing which is one piece with the wing clamping such that the forces generated by four pre-stressed piezoelectric stacks act as interior force couples between the ceiling of the housing and the prominent noses at wing root. The force transmitting struts are made from the same material as the wing model, as well as the excitation mechanism housing, for thermal extension reasons. Figure 6 also gives additionally some information about the technical data of the balance sensors and the piezoelectric stacks.

Figure 7. HIRENASD model in wind tunnel, showing markers for SPT on the pressure side. Slots in sidewall open

A surface pattern tracking optical system (SPT) using ultra high speed cameras and frame grabbers was installed for displacement measurement by means of optical marker tracing. The markers are placed on the pressure side of the wing for all model modifications, see Fig. 7. A high speed link for the frame transfer was established by ETW using fibre optic cables. New high power flash lights with an operating frequency up to 1kHz were designed in the project and installed by ETW for the SPT system. All experiments are performed in transonic flow with open slots in the side walls, as can also be seen in Fig. 7 on the side wall at the right.

The HIRENASD wing model had been equipped with 259 cryogenic miniature/ultra-miniature pressure sensors (Kulites) which were implemented in 7 span-wise sections in flow direction. The relative span positions η of these 7 sections are depicted in Fig. 8. Unfortunately not all, but 205 sensors were measuring correctly. On the right hand side of Fig. 8 the numbers of sensors which were functioning during the experiments are exemplarily presented for three measuring sections. In this context it must be mentioned, that in ref. 13, where the measuring techniques for HIRENASD was already described, a misprint had happened in Fig. 7 of ref. 13 with respect to the assignment of one pressure section.

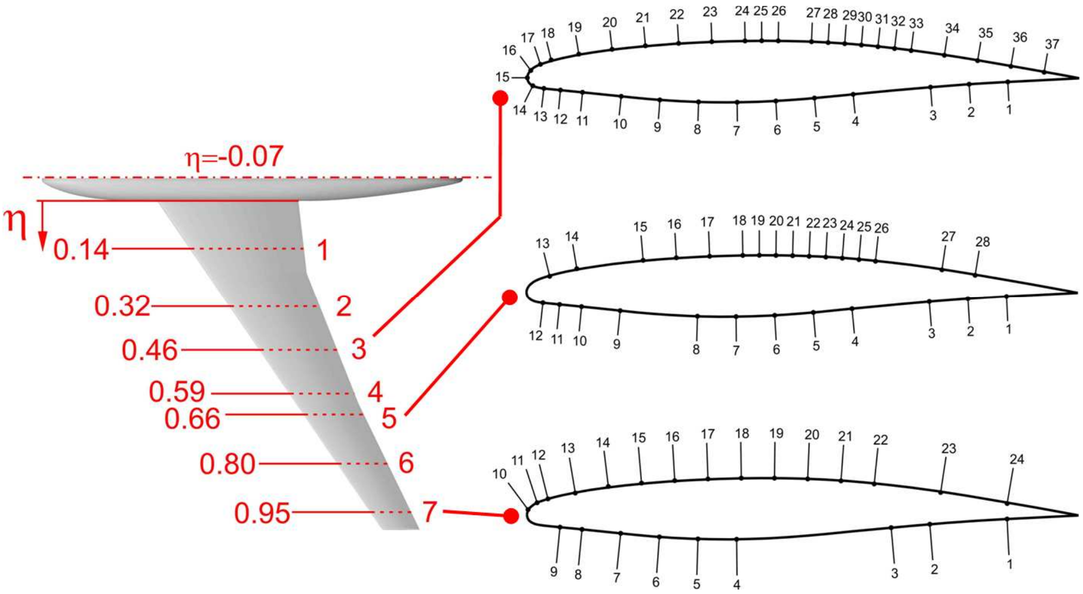

Figure 8. Pressure sensors distributed in 7 span-wise sections.

Furthermore, the wind tunnel model assembly was equipped with 28 strain gauges of which 6 were placed in the wing clamping at the excitation force transmitters and the other 22 were distributed inside the wing model. For monitoring acceleration during the tests several acceleration sensors were placed in the assembly, 11 from these accelerometers were implemented inside the model, all at the upper part of the wing model.

D. Test Envelopes

The European Transonic Wind tunnel is a cryogenic facility with closed circuit. The fluid is nitrogen gas. Flow conditions can be chosen as follows: fluid temperatures from 110K to 313K and the total pressure from 0.125MPa to 0.45MPa. The dimensions of the test section are height 2.0m, width 2.4m and length 9.0m. The nozzle is adjustable, walls in the measuring section can be chosen slotted or closed, and a second throat is present behind the test-section. Controlled liquid nitrogen injection and gaseous nitrogen blow-off maintain temperature and pressure at the chosen level and a two-stage 50MW compressor provides Mach numbers from Ma=0.15 to Ma=1.3. Mach number can be very quickly adjusted to a chosen value.

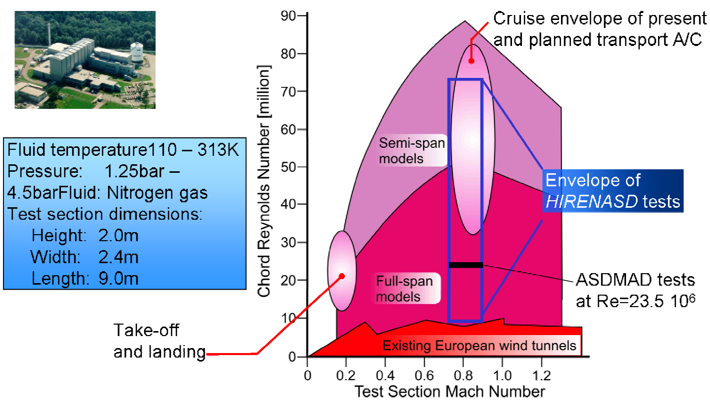

Figure 9. Range of test conditions in ETW

The turntable permits continuous change of angle of attack at low angular speed, e.g. 0.2deg/sec, such that static polars can be run in an angular sweep.

Under the lowest temperature condition and static pressure around 0.4MPa, it is possible in ETW to achieve Reynolds numbers of up to 80 millions in half-model testing at transonic Mach numbers, with the aerodynamic mean chord as reference length. One advantage of ETW is that the parameters Mach number, Reynolds number and dynamic pressure, or even more adequate, the ratio of dynamic pressure to Young's modulus of the model material, which are influencing the aero-elastic behaviour of the wing, can be varied independently of each other, see Fig. 9 and 10.

Test envelopes from HIRENASD and ASDMAD are presented in Fig. 10 for Mach number Ma=0.8. Conditions of test series of the HIRENASD project are presented in the envelope by numbers. The numbering corresponds to the sequence of the performed test series. During each series the values of q/E and Reynolds number are fixed. Series 1 to 3 were conducted with transition bands fixed at 12% chord on the body side section and at 15% chord on the two outer sections of the suction side, and continuously at 5% chord on the pressure side. Thereafter, the transition bands were removed for Reynolds numbers from 23.5 to 73 million. The ASDMAD test envelope concentrates on Reynolds number 23.5 10^6. Similar test polars as for Ma=0.8 were used for different Mach numbers from 0.7 to 0.88 for analyzing the effect of Mach number changes.

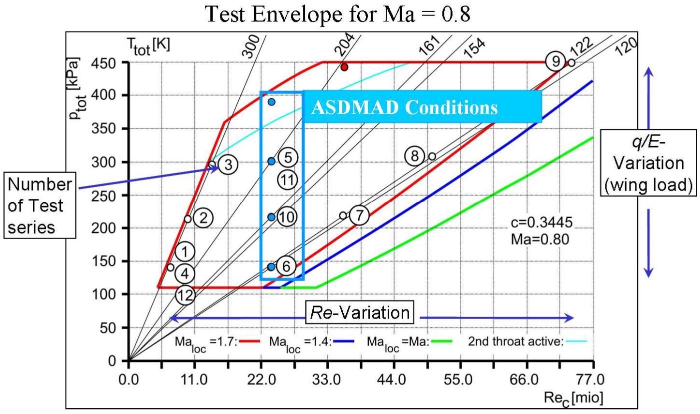

Figure 10. Test envelopes for HIRENASD and ASDMAD, Mach number Ma=0.8

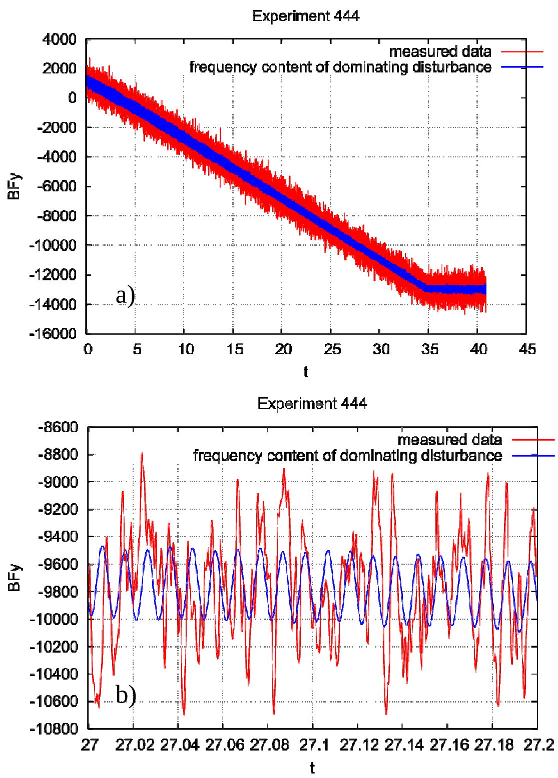

Figure 11.Wing normal force represented by raw data (a)). Zoom close to α=3° (b)).

III. Upstream Running Waves in Nominally or Quasi-Stationary Flow

A. Non-Stationary Content in Quasi-Stationary Polars

Stationary polars are performed in ETW in an α-sweep at low angular speed, as described above. The balance force data is recorded by ETW after passing a hardware filter at a frequency of about 5 Hz. The new piezoelectric balance permits high frequency data recording at e.g. 4 kHz in the HIRENASD tests or at 20 kHz as in the ASDMAD tests. That enables a much deeper insight in the content of possibly occurring unsteady processes in the quasi-stationary tests by means of dynamic analysis.

Indeed dynamic analysis of quasi-stationary experiments, i.e. tests without using the vibration excitation mechanism for defined excitation, reveals the presence of stochastic aerodynamic disturbances which excite the wing model for vibration in its natural modes. This has been discussed in ref. 16 where the focus was on stochastic non-stationary changes of the balance normal force component to the wing. As mentioned earlier, the angle of incidence α was changed very slowly, at a reduced frequency with c_{ref} as reference length in the order of magnitude of 10^{-6}, which is actually quasi-stationary. It was found that the first seven modes contain almost all stochastic influences[16].

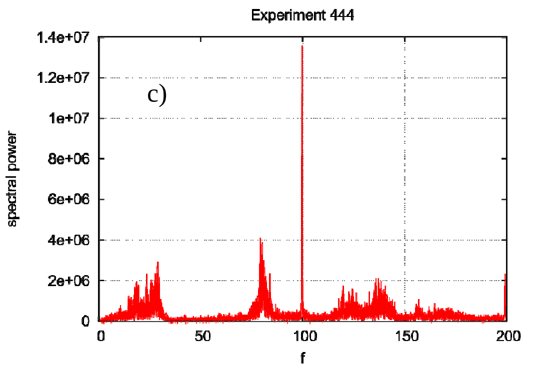

Figure 11 (cont.). Frequency spectrum derived from wing normal force data (c)).

The data registered by the implemented acceleration sensors during the observed unplanned excitation by stochastic disturbances has been used live in the experiments for determining the natural mode frequencies of the 1st, 2nd and 5th mode under wind on at the chosen wind tunnel conditions. This way the frequencies for vibration excitation close to resonance at the corresponding wind tunnel condition were defined.

Fourier analysis of the aforementioned force component revealed for HIRENASD tests another very high peak at a frequency which is not one of the natural modes of the elastic wing assembly. Figure 11 shows in the upper picture a) the normal force as recorded by the balance over time for the complete stationary polar in experiment no. 444 at Mach number Ma=0.75. The apparently very strong noise contains as one significant component this, with respect to the wing model, non-natural frequency, represented in blue color. The raw data are plotted in red. The content belonging to the "non-natural" frequency has been determined by narrow-band Fourier back-transformation. In the diagram b) underneath, a blow up of the diagram is shown for a very short time period at about angle of attack α=3°. The last diagram c) of Fig. 11 shows the spectral density with the highest peak slightly lower than 100Hz. This particular frequency can be detected for this experiment in almost all pressure sensors too. In the following section a close look into the raw data will be given to explain the observed phenomenon which appears as responsible for the large RMS values present in the stationary pressure distributions which were derived from the raw data by low pass filtering with 5Hz according to the ETW-own data acquisition system which uses a hardware filter.

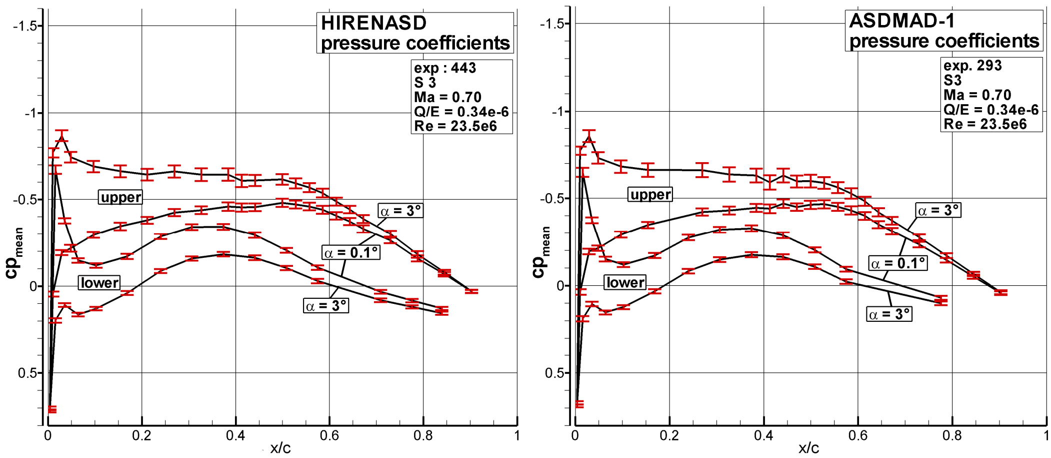

Figure 12.Mean pressure distribution in section 3 with local RMS values, Mach number Ma=0.7. Left: HIRENASD experiment no. 443. Right: ASDMAD-1 experiment no. 293

Figures 12 and 13 each show a comparison of low pass filtered pressure distributions in section 3 together with the RMS values for HIRENASD and ASDMAD-1 tests at the same wind tunnel conditions for two angles of attack α=0° and α=3°. Since pressure section 3 is not close to the winglet and the winglet is the only difference between the two configurations, results should be approximately the same. In Fig. 12 results for Mach number Ma=0.7 are depicted for comparison. Indeed one observes only little differences of the RMS values, in contrast for Ma=0.8 in Fig. 13 where the HIRENASD experiment exhibits much larger RMS values. The largest extent of strong disturbances over chord was found in the HIRENASD tests for Ma=0.75. This statement holds for all Reynolds numbers and wing load conditions of the HIRENASD tests and is exemplarily presented in Fig. 14.

The "non-natural" frequencies could be observed in all quasi-stationary HIRENASD experiments with Mach numbers Ma= 0.7 to 0.8 with values depending solely on the speed of sound at the free-stream conditions in the wind tunnel flow. It is remarkable, that these frequencies did not regularly appear in the ASDMAD-1 tests.

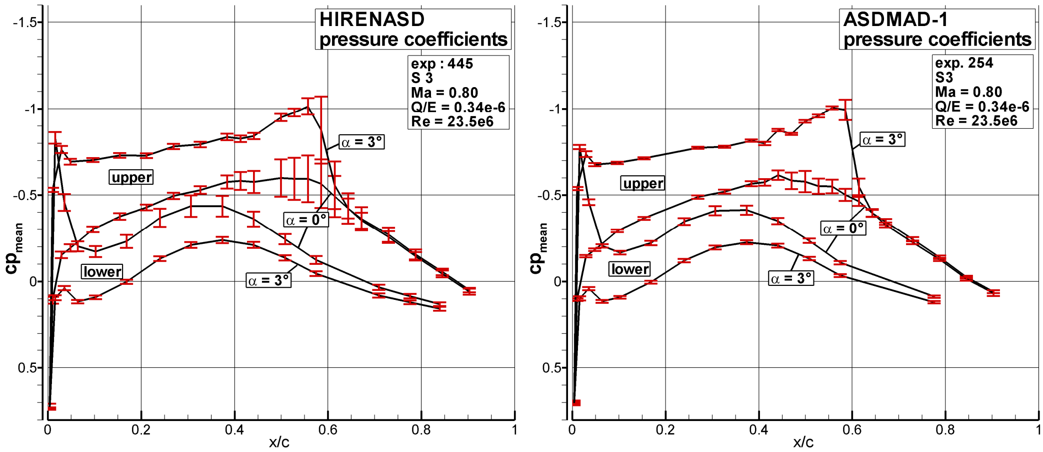

Figure 13.Mean pressure distribution in section 3 with local RMS values, Mach number Ma=0.8.

B. Upstream travelling pressure waves

The time behaviour of the raw data from the pressure sensors indicate that small amplitude pressure waves start periodically at the trailing edge and move upstream. This type of waves has first been experimentally analyzed in ref. 5 and had also been observed in DNS simulations reported in ref. 6 and in the HIRENASD pre-tests with a BAC 3-11 airfoil in KRG Göttingen as pointed out in the introduction.

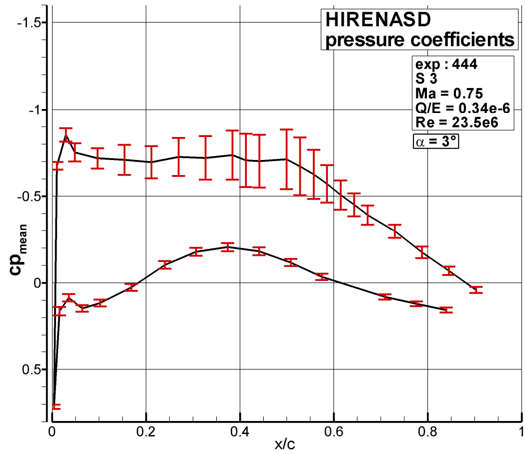

Figure 14.Mean pressure in section 3 with local RMS values, Mach number Ma=0.75

The experimental observation from the raw HIRENASD pressure data of experiment number 249 with oncoming flow at Ma=0.75 is exemplarily depicted for pressure section 3 in Fig. 15 in a perspective view over a time period of 40 milliseconds. For this purpose, the wing profile has been represented in its flat projection whereby the upper part represents the pattern on the pressure side and the lower part that on the suction side. The perspective view shows the very nicely organized wave pattern where in this case upstream running waves start with a frequency of about 112 Hz which again only depends on the speed of sound of the oncoming flow for the respective wind tunnel condition. For angle of attack α=0° the flow speed exceeds on the suction side of the wing locally Ma=1.0 very little. The amplitudes of the waves in that case are higher than for lower angles of attack. The waves steepen while running upstream and disappear where the local Mach number undercuts the value Ma=1 in the front part of the wing section. For α=3° the supersonic regions have much greater extent, and the waves starting at the trailing edge steepen to upstream running shocks, which weaken approaching the leading edge and finally disappear. That happens periodically with the aforementioned non-natural-mode frequency. When the fore-running shock is not yet vanished the follower shock has already formed in the mid part of the suction side. One observes two transient local supersonic regions at the same time, one in the front part and one in the mid part of chord (see middle and left picture of Fig. 15). The fingerprint of the transient supersonic space-time domains in the right picture of Fig. 15 confirms this observation.

The forming and upstream running of shock waves occurs in all pressure sections as can be seen in Fig. 16. Periodicity with time is also the same in all sections. Looking in span-wise direction, the shocks in the different sections have different running distances due to the different extent of the transient supersonic region in the 7 sections over span and do apparently not form single continuous wave fronts over span.

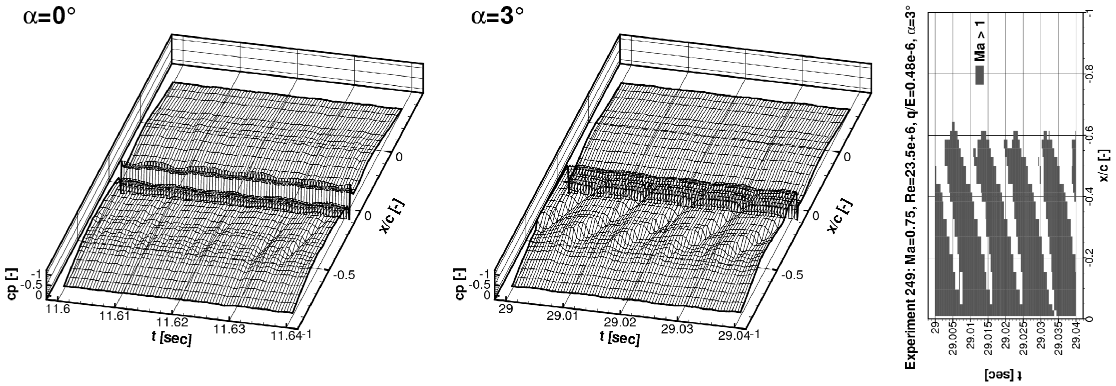

Figure 15.Upstream running pressure waves contained in raw pressure data, Ma=0.75

The behaviour of the pressure coefficient behind the final shock does not seem to be heavily alternated for the different stations passed by the upstream running shock. Apparently only weak flow separation occurs, although the wave pattern seems to be driven or at least triggered by disturbances in the boundary layer arriving from the trailing edge at the rear part of the transient supersonic region. Therefore, the observed phenomenon does not exhibit classical shock buffet properties. Best insight into the phenomenon is achieved by observing the wave pattern in a movie made from unfiltered pressure data.

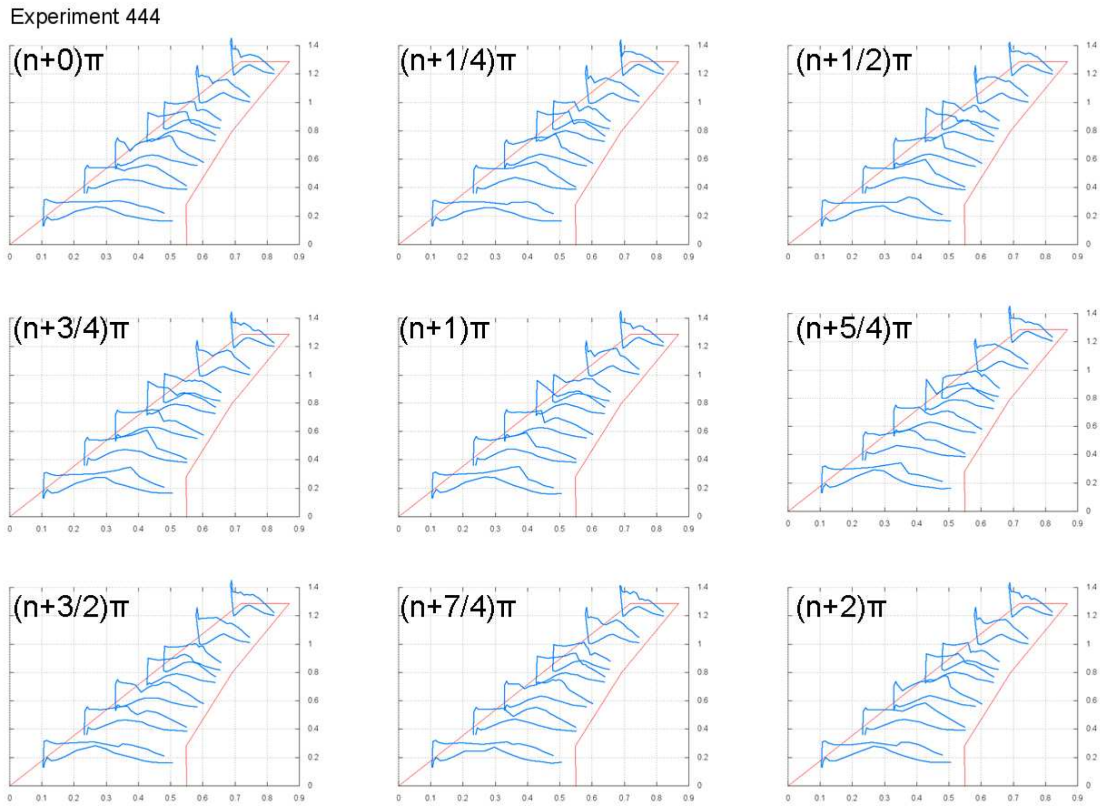

Figure 16.A full cycle of the non-natural frequency showing the upstream running pressure waves in all pressure sections.

IV. Results from Forced Vibration

A. Vibration Excitation Close to Resonance

The above mentioned stochastic excitation of wing vibration during quasi-stationary experiments (section III. A.) has been used to determine mode frequencies at the respective wind tunnel conditions on the basis of accelerometer measurement data. An example can be seen in Fig. 17 where the accelerometer at the position 13(1) was used to establish a Fourier spectrum. It shows clearly the peaks of the 1st bending, 2nd bending and 1st torsion, while the narrow peak at about 130Hz corresponds to the so-called non-natural frequency as described above. The right diagram in Fig. 17 illustrates how the spectra deliver also information about aerodynamic damping.

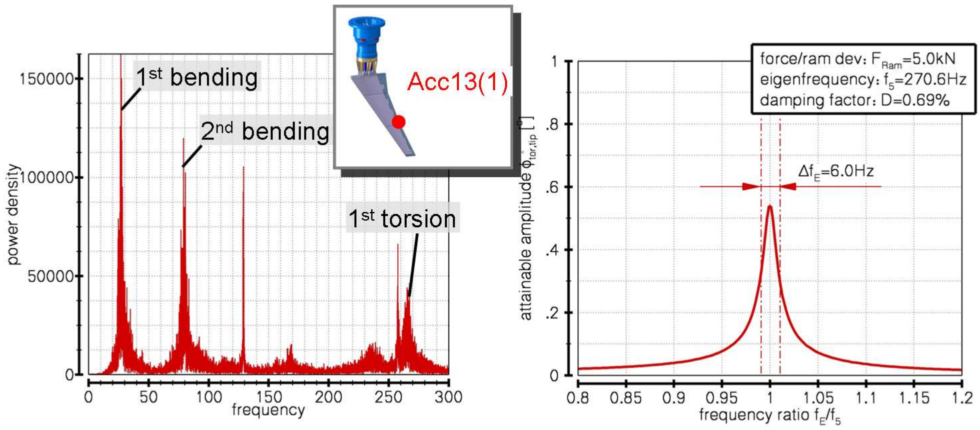

Figure 17.Extraction of information about natural modes of the wing from stochastic excitation in quasi-stationary HIRENASD experiments.

B. Data Reduction

The recorded measurement data in dynamic tests with defined vibration excitation exhibit considerable noise including disturbances caused by aerodynamic effects. The results of measurements presented in this paper are outcomes of a band filtering process based on Fourier analysis[16]. Discrete Fourier transform has been applied to the raw data, followed up by back-transformation within frequency bands around the frequencies which are of special interest. In case of vibration excitation with a defined frequency, an appropriate frequency band width has been elaborated using the data record of the control voltage in the piezoelectric stacks of the excitation mechanism as a reference, which is very clean from disturbances and must not be degraded applying the filtering process on it. After finding out the maximum of admissible band width which fulfils this requirement, the upper limit of the filter band width has been defined. As an example, Fig. 18 shows the comparison of the unfiltered and filtered data record of the control voltage in the two upper diagrams on the right of the figure and the unfiltered and filtered data of the measured balance force in normal direction to the wing plane. The results presented in this figure belong to the experiment no. 346 within which predominantly the 2nd mode was being excited at a frequency of 83.3 Hz. Mach and Reynolds numbers were Ma=0.85 and Re=23.5 10^6. The angle of attack corresponds to no lift under stationary conditions and was measured α=-1.33° at the turntable.

Figure 19 shows for experiment no. 346 a result of the pressure distribution in pressure section 7 during about 4 periods in the fully excited vibration state which would exhibit pressure distributions varying periodically and smoothly at constant amplitudes in an ideal case. In the experimental reality, that does not apply due to disturbances. The recorded measurement data behave non-smoothly as can be seen in the upper pictures of Fig. 19 where the unfiltered measurement data is presented for the suction side of the wing on the left and for the pressure side on the right as recorded in the experiment no. 346.

At Mach number Ma=0.85 and angle of attack α=-1.33° three supersonic regions, which are each closed by a shock on their downstream side, are present and changing in position and strength during the vibration. One shock is present on the upper side of the wing in the pressure section referred to, while two shocks are established on the lower side, of which one results from the special shape of the BAC 3-11 profile which exhibits a very strong positive curvature near the leading edge. This is followed by a small interval with negative curvature until the flow reaches again a region with positive surface curvature. There, behind the thickness maximum the second shock closes the second supersonic region on the pressure side, for no lift at Ma=0.85.

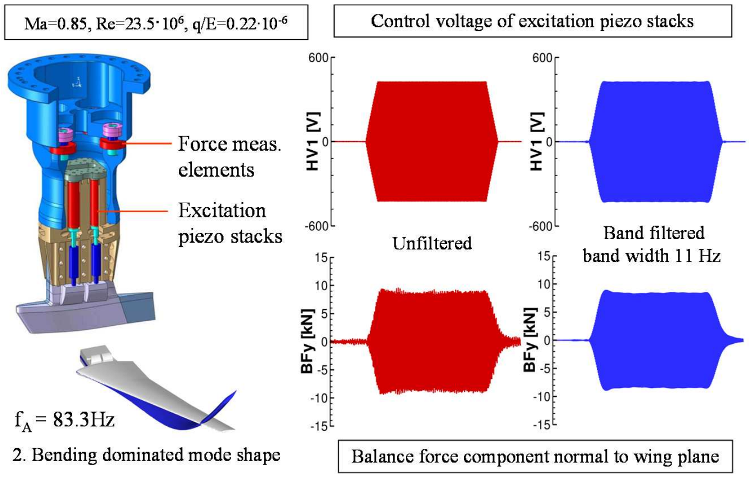

Figure 18.Experiment 346. Example for processing of measured data applying band filtering based on Fourier analysis. α=-1.33° (no lift), excitation with 2nd mode frequency 83.3Hz.

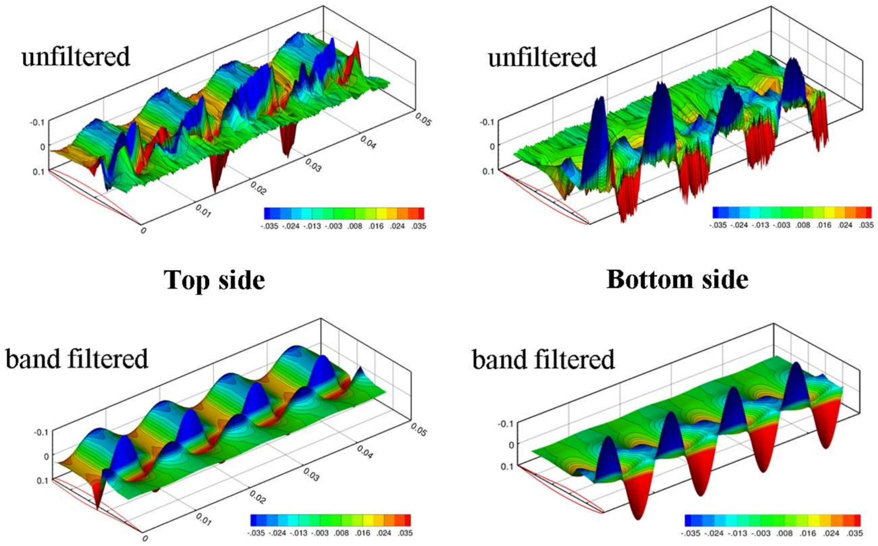

Figure 19.Experiment 346, Ma=0.85, Re=23.5 10^{6}, q/E=0.22 10^{-6}, α=-1.33° (no lift). Excitation frequency 83.3Hz. Raw data (pictures on top) and band filtered data (pictures beneath). Left: Suction side, right: Pressure side of the wing model.

The filtering process using a band width of 11Hz yielded the results presented in the pictures on the bottom of Fig. 19. All shocks are well represented including their changes in amplitude and position. The loss of magnitude in the pressure variation compared to the unfiltered data is actually not only caused by noise in the usual sense, its main part seems to be caused by aerodynamic disturbances occurring in the experiments already mentioned above.

Further results of this section are concerning measured pressure distributions after band-filtering which are presented in terms of real and imaginary parts using the mean of amplitudes of pressure data during excitation and their phase angles relative to acceleration data at position 13(1). This reference between pressure data and an acceleration sensor has been introduced to provide data for numerical code validation in the sense of a transfer function. Figure 20 shows the real and imaginary parts for the four outermost pressure sections of experiment no. 346. Strong pressure fluctuations and oscillating shocks related to excitation are responsible for the peaks in the real and imaginary parts of the transfer function.

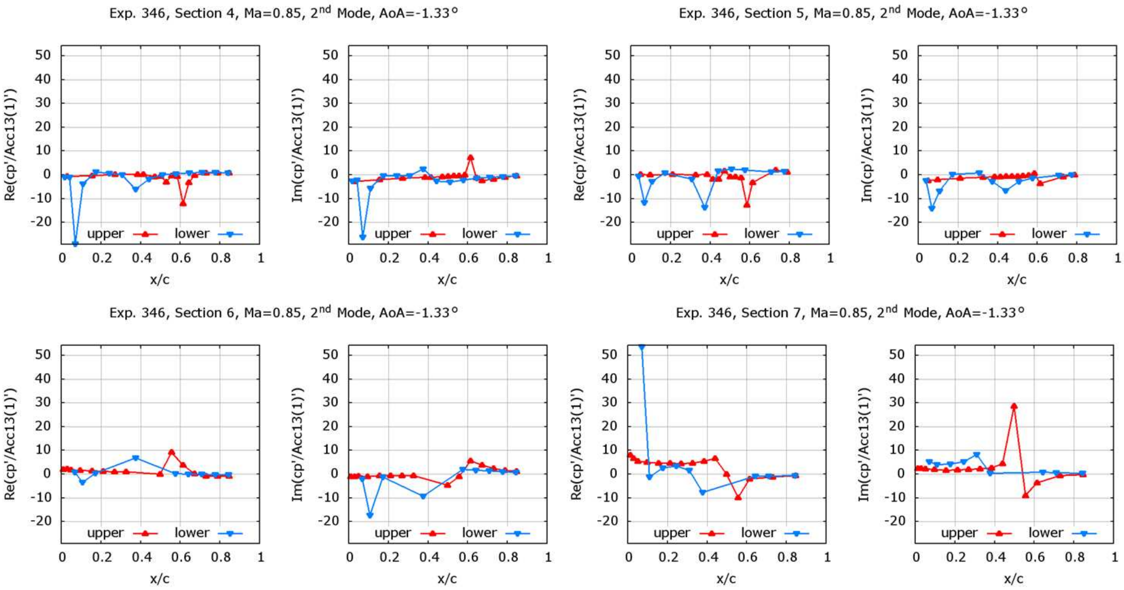

Figure 20.Real and imaginary parts of normalized pressure variations in sections 4 to 7 due to excited vibration close to resonance with the 2nd natural frequency. Re=23.5M, q/E=0.22 10^{-6}.

C. Influence of Reynolds number on ASD response in experiments with excited vibration

In this section dynamic experiments at Reynolds number $Re=23.5\cdot10^6$ with natural transition at the model leading edge are considered in comparison to experiments at $Re=7\cdot10^6$ with artificial transition to turbulent flow close to the leading edge. Mach number is Ma=0.85, the aerodynamic load factor is $q/E=0.22\cdot10^{-6}$ in all compared cases as well as the no lift condition at $\alpha=-1.27°$ for $Re=7\cdot10^6$ and $\alpha=-1.33°$ for $Re=23.5\cdot10^6$. The related experiments are the test runs no. 148 and 342 for the 1st mode and no.163 and 346 for the 2nd. Figure 21 shows mean pressure distributions from HIRENASD experiments no.148 and 342 in pressure sections 4 to 7 for both values of Reynolds number and reveals that the curves are obviously approximately coincident. The same holds for the means of the other compared experiments. But for the dynamic constituents of the pressure distributions that is different, as can be seen in Fig. 22 and Fig. 23 for both excitation frequencies. There one can recognize that differences in amplitude and particularly in phase occur. This fact is first a convincing argument that introducing artificial transition in aero-elastic experiments at low Reynolds number can not replace aero-elastic experiments at high Reynolds numbers with natural transition. But it is also important in practice when the critical question is to be answered, if the wing takes energy for vibration from the fluid or if its vibration is damped.

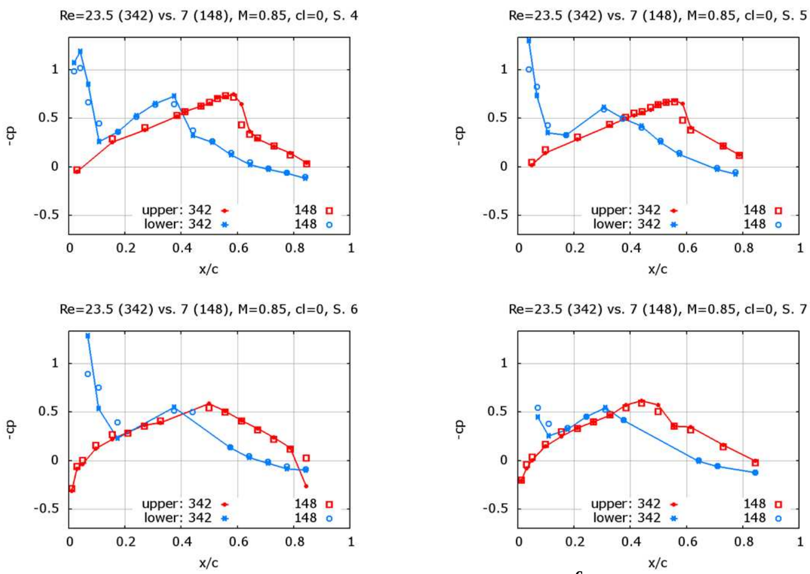

Figure 21.Averaged pressure coefficient for Re=7 10^6 with artificial transition and Re=23.5 10^6 with natural transition. Zero lift condition, q/E=0.22 10^{-6}.

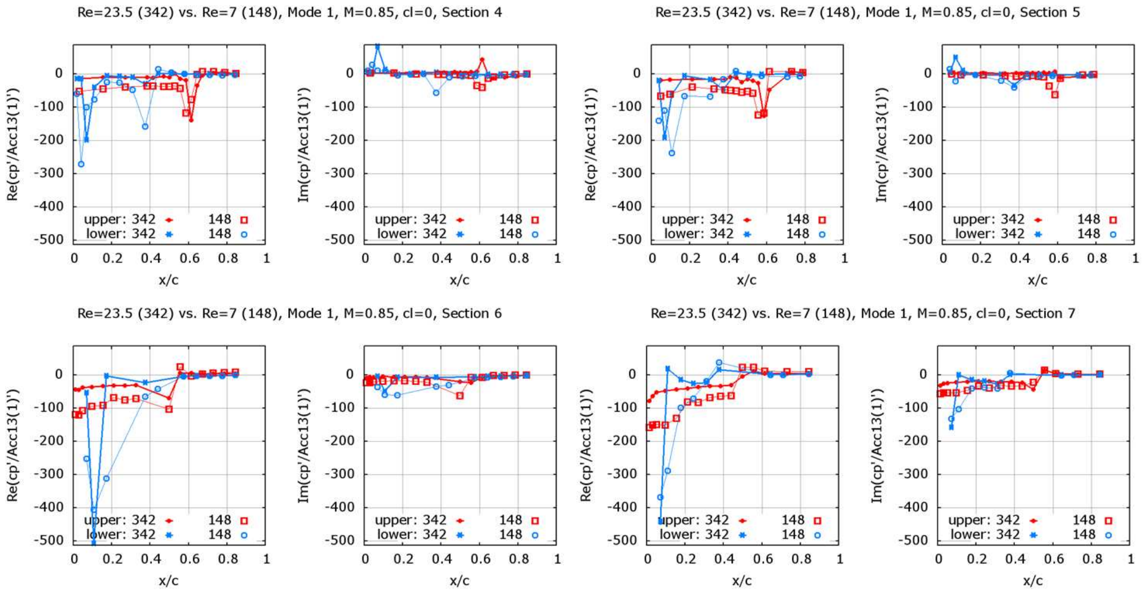

Figure 22.Real and imaginary parts of normalized pressure variations in sections 4 to 7 due to excited vibration close to resonance with the 1st natural frequency for Re=7 10^6 with artificial transition and Re=23.5 10^6 with natural transition. Zero lift condition, q/E=0.22 10^{-6}.

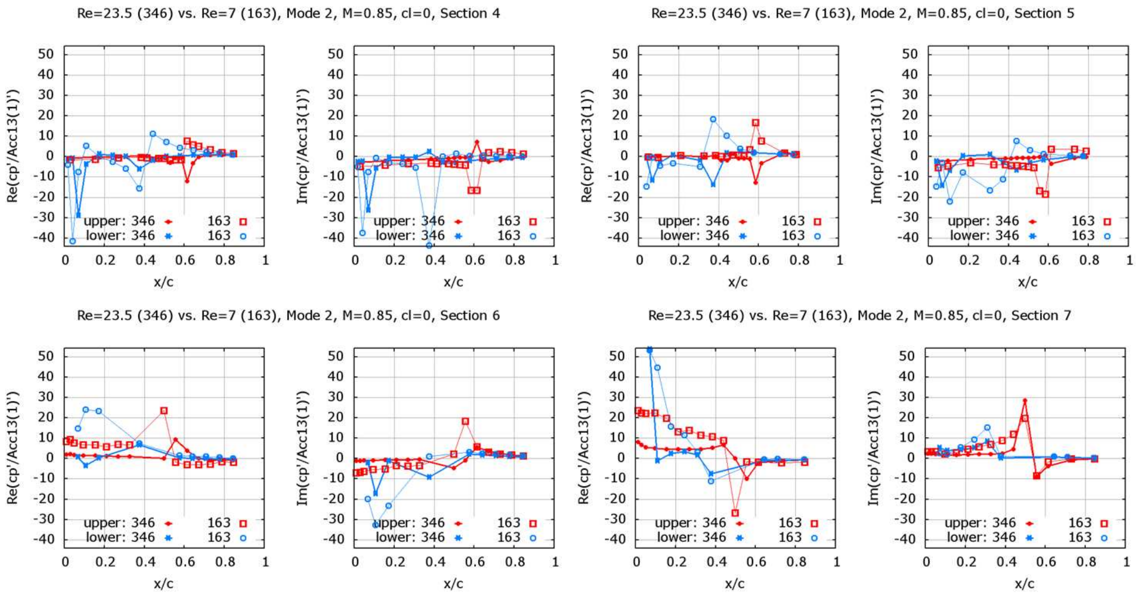

Figure 23.Real and imaginary parts of normalized pressure variations in sections 4 to 7 due to excited vibration close to resonance with the 2nd natural frequency for Re=7 10^6 with artificial transition and Re=23.5 10^6 with natural transition. Zero lift condition, q/E=0.22 10^{-6}.

D. First Results of Dynamic ASDMAD-1 Experiments with Excited Vibration

Results from non-stationary constituents during tests with excited vibration in the ASDMAD-1 campaign and in the HIRENASD project are also shown in comparison for the same wind tunnel conditions as in the section above on HIRENASD experiment no. 346. Raw data has been treated the same way as described for the HIRENASD experiments in the initial sections above. The results for the real and imaginary parts of the periodically changing pressure distributions in sections 3, 4, 5 and 6 during fully excited vibration close to resonance are shown for the first natural mode in Fig. 24 and for the second natural mode in Fig. 25. Apparently the presence of the winglet does not drastically change the characteristics of the system response to excited vibration.

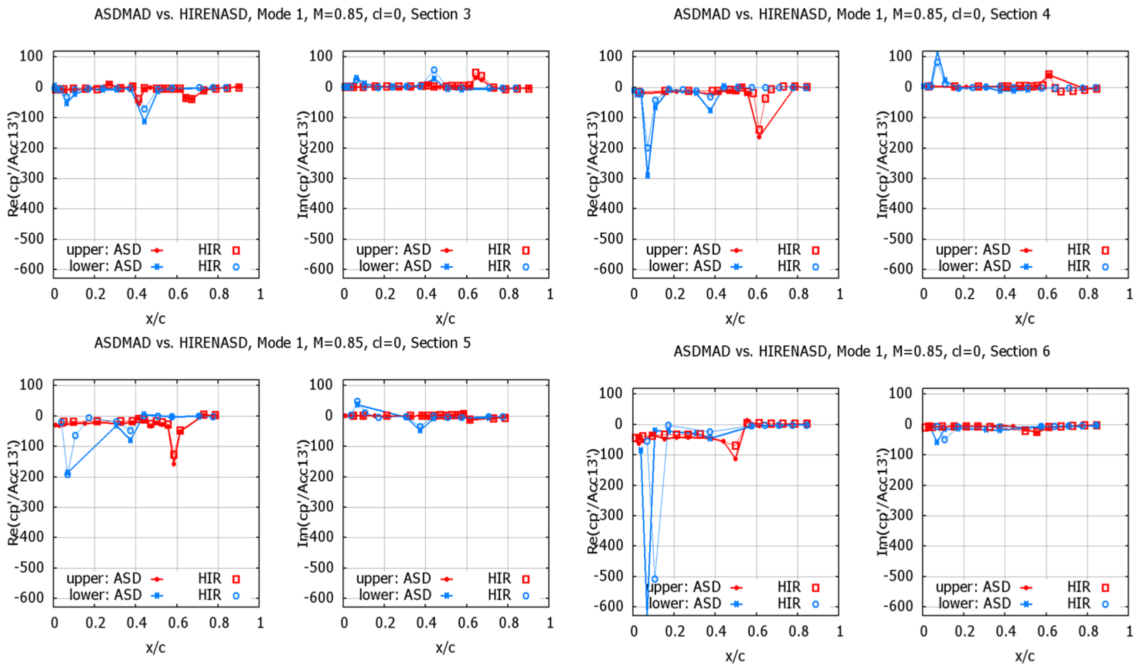

Figure 24.Real and imaginary parts of normalized pressure variations in sections 3 to 6 due to excited vibration close to resonance with the 1st natural frequency comparing ASDMAD-1 with HIRENASD. Re=23.5M, q/E=0.22 10^{-6}.

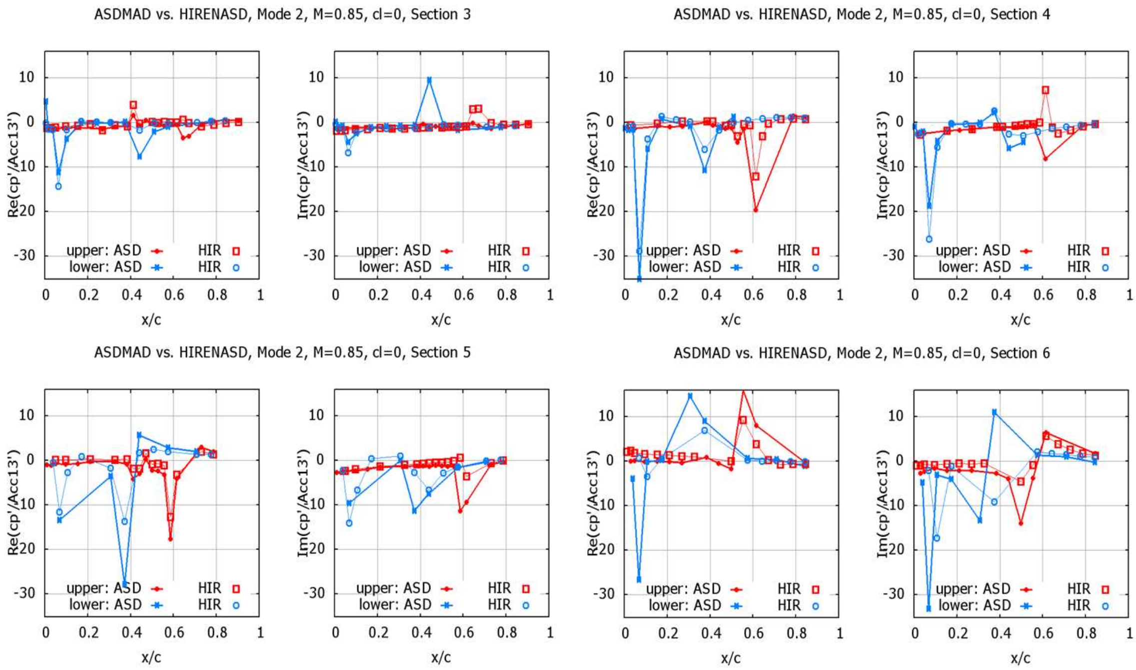

Figure 25.Real and imaginary parts of normalized pressure variations in sections 3 to 6 due to excited vibration close to resonance with the 1st natural frequency comparing ASDMAD-1 with HIRENASD. Re=23.5M, q/E=0.22 10^{-6}.

V. Conclusions

Selected quasi-stationary and dynamic experiments with excited vibration have been considered. A close look into the raw data of the stationary HIRENASD experiments revealed upstream running small amplitude pressure waves in the subsonic regions of the wing surface. For flow conditions with incipient supersonic regions the pressure waves may first steepen running upstream and disappear approaching the leading edge. For Mach number Ma=0.75 stronger upstream running shock waves have been detected. The process is periodical with time and its frequency only depends on the free-stream speed of sound. It happens periodically as well, that two transient supersonic regions are present in a wing section. The small amplitude pressure waves appeared also in the ASDMAD tests for the wing model with rigid winglet. But a particular frequency was not anymore seen. The phenomenon appears to be more like noise.

The analysis of Reynolds number influence for turbulent flow with artificial and turbulent flow with natural transition resulted in the statement that larger phase differences occurred in the pressure fluctuation response to excited vibration, whilst the stationary mean pressure distributions approximately coincided. Therefore, one has to be careful to draw conclusions for self-excited vibrations from low Reynolds number flow with artificial transition.

In the evaluation of the dynamic tests it was found that the unsteady flow processes caused by excited vibration behave approximately in a comparable manner for the clean HIRENASD wing and the ASDMAD-1 wing.

Acknowlegdments

Authors are very grateful to the German Research Foundation (DFG) for funding the HIRENASD project and co-funding the ASDMAD project and thank Airbus Germany for providing financial support for the development of the piezoelectric wind tunnel balance and partnership in ASDMAD, ETW for providing wind tunnel adaptations for dynamic measurements and giving continuously advice during the model preparations and conduction of the experiments.

References

[1]Ballmann J. (Ed.): "*Flow Modulation and Fluid-Structure Interaction at Airplane Wings*". Notes On Numerical Fluid Mechanics and Multidisciplinary Design, Vol. 84, Springer, 2003

[2]Cole, S.R., Noll, T.E., Perry, B. III: "Transonic Dynamics Tunnel Aeroelastic Testing in Support of Aircraft Development". *Journal of Aircraft*, Vol. 40, No. 5,pp. 820-832, 2003.

[3]Bartels, R.E., Edwards, J.W.: "Cryogenic Tunnel Pressure Measurements on a Supercritical Airfoil for Several Shock Buffet Conditions". NASA TM-110272, 1997

[4]Ballmann, J., "HIRENASD technical reference" (online database), http://www.lufmech.rwth-aachen.de/HIRENASD/

[5]Tijdeman, H., "Investigation of the Transonic Flow around Oscillating Airfoils", National Aerospace Lab., NLR TR-77090, Amsterdam, Oct. 1977.

[6]Klioutchnikov, I., Ballmann, J.: "DNS of Transitional Transonic Flow about a Supercritical BAC3-11 Airfoil using High-Order Shock Capturing Schemes", *Direct and Large Eddy Simulation VI*. Springer Netherlands, pp.737-744, 2006

[7]Hermes, V., Klioutchnikov, I., Alshabu, A., Olivier, H.: "Investigation of Unsteady Transonic Airfoil Flow", *46th AIAA Aerospace Sciences Meeting and Exhibit*, Reno, Nevada, Jan. 7-10, 2008, AIAA 2008-627

[8]Alshabu, A., Olivier, H.: "Unsteady Wave Phenomena on Supercritical Airfoil", *AIAA Journal*, Vol. 46, no. 8, pp. 2066-2073, 2008

[9]Özger, E., Schell, I., Jacob, D.: "On the Structure and Attenuation of an Aircraft Wake". *AIAA Journal of Aircraft*, Vol. 38, No. 5, pp. 878-887, 2001

[10]Moir, I.-R.M.: "Measurements on a two-dimensional aerofoil with high-lift devices", AGARDAR-303, Vol. II, 58-59, 1994

[11]Reimer, L., Ballmann, J., Behr, M.: "Computational analysis of high Reynolds number aerostructural dynamics (HIRENASD) experiments", *International Forum on Aeroelasticity and Structural Dynamics (IFASD)*, Paper IFASD-2009-130, Seattle, 22-24 June 2009.

[12]Chen, B.-H., Brakhage, K.-H., Behr, M., Ballmann, J.: "Numerical simulations for preparing new ASD experiments in ETW with a modified HIRENASD wing model", *International Forum on Aeroelasticity and Structural Dynamics (IFASD)*, Paper IFASD-2009-131,Seattle, 22-24 June 2009

[13]Ballmann, J., Dafnis, A., Korsch, H., Buxel, C., Reimerdes, H.-G., Brakhage, K.-H., Olivier, H., Braun, C., Baars, A., Boucke, A.: "Experimental Analysis of High Reynolds Number Aero-Structural Dynamics in ETW", *46th AIAA Aerospace Sciences Meeting and Exhibit*, Reno, 7.-10. Jan 2008, AIAA 2008-841

[14]Dafnis, A., Buxel, C., et.al.: „Stationäre und Instationäre Untersuchungen an einem Elastischen Flügelmodell mit Winglet im Kryogenen Windkanal im Rahmen des ASDMAD-Projektes", *Deutscher Luft- und Raumfahrtkongress*, DLRK, 2010

[15]Korsch, H., Dafnis, A., Reimerdes: "Dynamic Qualification of the HIRENASD Elastic Wing Model", *Aerospace Science and Technology,* Volume 13, Issues 2-3, pp 130-138, 2009

[16]Ballmann, J., Boucke, A., Reimer, L., Dickopp, C.: "Results of Dynamic Experiments in the HIRENASD Project and Analysis of Observed Unsteady Processes", *International Forum on Aeroelasticity and Structural Dynamics (IFASD)*, Paper IFASD-2009-103, Seattle, USA, 2009